Issue on Microwave Circuit Aspects of Avalanche-Diode and Transferred Electron Devices), vol. MTT-18, pp. 890–897, Nov. 1970.
[2] S. Nagano and H. Kondo, "Highly stabilized half-watt IMPATT oscillator," *IEEE Trans. Microwave Theory Tech. (Special Issue on Microwave Circuit Aspects of Avalanche-Diode and Transferred Electron Devices)*, vol. MTT-18, pp. 885–890, Nov. 1970.
[3] K. Kohiyama and K. Momma, "A new type of frequency-stabilized Gunn oscillator," *Proc. IEEE* (Corresp.), vol. 59, pp. 1532–1533, Oct. 1971.
[4] E. F. Scherer, "Large-signal operation of avalanche-diode amplifiers," *IEEE Trans. Microwave Theory Tech. (Special Issue on Microwave Circuit Aspects of Avalanche-Diode and Transferred Electron Devices)*, vol. MTT-18, pp. 922–932, Nov. 1970.
[5] C. W. Lee and W. C. Tsai, "High power GaAs avalanche diode amplifiers," in *IEEE Int. Conv., Dig. Tech. Papers*, Mar 1971, pp. 368–369.
[6] M. E. Hines, "Special problems in IMPATT diode power amplifiers," in *1972 IEEE Int. Solid-State Circuits Conf. Tech. Papers*, Feb. 1972, pp. 34–35.
[7] H. Komizo, Y. Ito, H. Ashida, and M. Shinoda, "A 0.5-W CW IMPATT amplifier for high-capacity 11 GHz radio-relay equipment," in *1972 IEEE Int. Solid-State Circuits Conf. Dig. Tech. Papers*, Feb. 1972, pp. 36–37.
[8] W. C. Tsai, F. J. Rosenbaum, and L. A. MacKenzie, "Circuit analysis of waveguide-cavity Gunn-effect oscillator," *IEEE Trans. Microwave Theory Tech. (Special Issue on Microwave Circuit Aspects of Avalanche-Diode and Transferred Electron Devices)*, vol. MTT-18, pp. 808–817, Nov. 1970.
[9] D. C. Hanson and J. E. Rowe, "Microwave circuit characteristics of bulk GaAs oscillator," *IEEE Trans. Electron Devices (Second Special Issue on Semiconductor Bulk Effect and Transit-Time Devices)*, vol. ED-14, pp. 469–476, Sept. 1967.
[10] E. W. Sard, "A new procedure for calculating varactor Q from impedance versus bias measurements," *IEEE Trans. Microwave Theory Tech.*, vol. MTT-16, pp. 849–860, Oct. 1968.
[11] J. W. Gewartowski and J. E. Morris, "Active IMPATT diode parameters obtained by computer reduction of experimental data," *IEEE Trans. Microwave Theory Tech.*, vol. MTT-18, pp. 157–161, Mar. 1970.

Intermodulation Characteristics of X-Band IMPATT Amplifiers

ROBERT J. TREW, NINO A. MASNARI, AND GEORGE I. HADDAD

Abstract—**The intermodulation products produced when two equal-amplitude signals are applied to the input of an X-band IMPATT-diode amplifier have been measured. An Si p^+nn^+ IMPATT diode was operated in a double-slug-tuned coaxial reflection amplifier circuit that was tuned to provide 20 dB of small-signal gain at 9.340 GHz. The intermodulation tests consist of measurements of the magnitudes and frequencies of the amplifier output signals as a function of the input-signal drive levels and frequency separations. The gain and single-frequency characteristics of the amplifier were also measured, and are used along with the theoretical device and circuit admittance characteristics as a basis for explanation of the intermodulation results. A low-frequency dominance mechanism is found to exist in which the low-frequency signals are amplified more than the high-frequency signals. This mechanism becomes more significant as the amplifier drive level is increased.**

Introduction

As a result of the inherent nonlinearity associated with large-signal operation of avalanche transit-time devices [1], the introduction of two or more nonharmonically related signals into the input of an IMPATT amplifier results in the generation of intermodulation signals in the amplifier output. The distortion mechanism resulting from the production of these signals reduces the available power levels at the amplifier fundamental frequencies [2]. Measurements have been made of the intermodulation products generated when two equal-amplitude signals are applied to the input of an X-band IMPATT-diode amplifier.

The test results consist of measurements of amplifier output signals as a function of input-signal power levels and frequency separations. The results presented are typical for IMPATT-diode amplifiers. In particular, diodes fabricated at the Electron Physics Laboratory of the University of Michigan, as well as commercially available diodes, were tested and yielded similar results. Use is made of the IMPATT device and circuit admittance characteristics to explain the output behavior of the amplifier.

Circuit Description

The block diagram of Fig. 1 represents the basic reflection amplifier circuit used in these experiments. Input–output signal separation is provided by a coaxial three-port circulator. Amplifier tuning is accomplished through the positioning in the resonant cavity of two 20-Ω copper tuning slugs; one being $\lambda/4$ at 8 GHz, the other $\lambda/4$ at 10 GHz. The diode is located at the end of the resonant cavity and is kept at an approximately constant temperature by a water-cooled heat sink. The two source signals are amplified for large-signal operation and are introduced into the amplifier input through a "magic-T" that insures source signal isolation. The primary measurement circuit consists of a precision

Manuscript received April 28, 1972; revised August 16, 1972. This work was supported by the National Aeronautics and Space Administration under Grant NGL 23-005-183. This paper was presented at the 1972 International Microwave Symposium, Chicago, Ill., May 22–24, 1972.

The authors are with the Electron Physics Laboratory, Department of Electrical and Computer Engineering, the University of Michigan, Ann Arbor, Mich. 48104.

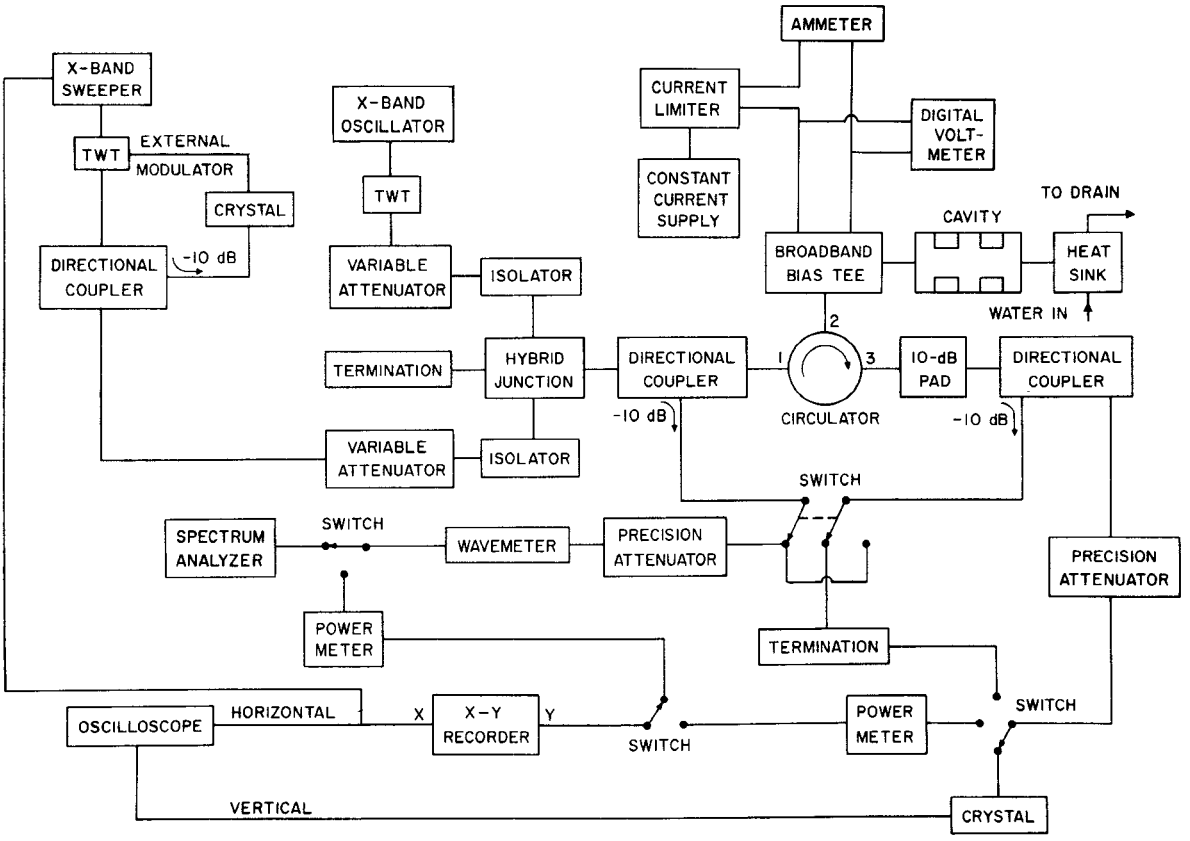

Fig. 1. Reflection amplifier circuit, two-frequency operation.

attenuator/spectrum analyzer combination calibrated with an external source to read power levels at the input–output plane of the resonant cavity. A cavity wavemeter is used to provide accurate signal frequency determination.

Discussion

The basic single-frequency operation of IMPATT amplifiers has been discussed by Laton and Haddad [3] and is reviewed here for convenience. Fig. 2 shows a typical admittance plot of an IMPATT device and a plot of the negative of the admittance of a one-slug-tuned reflection amplifier circuit for a stable circuit tuning condition. The power gain of a reflection amplifier can be expressed as [3]

$$\text{power gain} = |\Gamma|^2 = \left| \frac{Y_{\text{circuit}} - Y_{\text{device}}^*}{Y_{\text{circuit}} + Y_{\text{device}}} \right|^2$$

where

Γ the reflection coefficient;
Y the admittance.

According to this expression, a necessary condition for stable amplification is the nonintersection of the diode admittance and circuit negative-admittance curves at a common-frequency point. The denominator of the power-gain expression represents the distance between common-frequency points on the circuit and

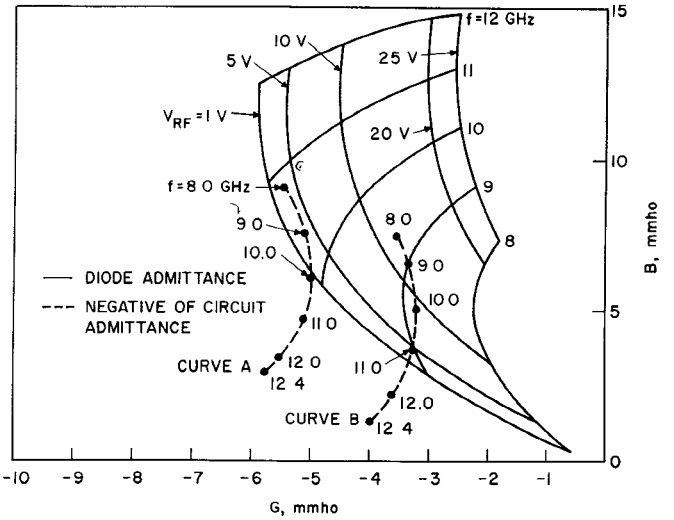

Fig. 2. The diode admittance for different values of V_{RF} and frequency, and the negative of the circuit admittance versus frequency at the plane of the diode wafer.

diode curves. The intersection of the curves at a common frequency would produce a denominator of zero value, and thus could result in infinite gain and oscillation at the frequency of the point of intersection. It follows that the magnitude of the power gain possible for any tuning condition is dependent upon the distance between common-frequency points on the diode and circuit negative-admittance curves. For a fixed slug position, where the amplifier is tuned for maximum gain

occurring with small-signal operation, it is expected that an increase in the operating power level will result in a decrease in gain. The increased power level causes a shift in the diode operating point that results in an increased distance between common-frequency points on the device and circuit admittance curves, thereby increasing the denominator value of the power-gain expression and thus reducing the gain. An increase in operating power level is also expected to result in a decrease in the frequency at which maximum gain occurs. Basically, this is due to an increasing device susceptance with increasing power level which reduces the resonant frequency of the amplifier–circuit interaction [4].

Since the large-signal operation of IMPATT amplifiers is nonlinear, multifrequency operation results in the generation of sum-and-difference intermodulation products in the amplifier output. It is expected that the lowering of the gain and its corresponding frequency with increasing drive levels will affect the magnitudes of the intermodulation as well as fundamental signals. Increasing the drive level should result in a low-frequency dominance mechanism in which the low-frequency signals are amplified more than the high-frequency signals. It is also expected that the intermodulation products will reduce the power available at the fundamental signals.

Spurious Oscillations

The circuit characteristic identified as curve *A* in Fig. 2 is somewhat idealized in that it allows for stable amplification at all frequencies, regardless of the power level to which the diode is driven. A more typical characteristic would be one that in some manner "passed" through the diode admittance curves (e.g., curve *B* in Fig. 2), thus allowing the curves to intersect at common-frequency points at certain drive levels. This would, of course, result in in-band spurious oscillations occurring as the drive level is increased. Spurious oscillations can also be induced at frequencies below the avalanche frequency of the IMPATT device at high RF drive levels. Basically, this phenomenon is attributed to a parametric mechanism in which oscillations at the IMPATT frequency induce negative conductance at subharmonic frequencies and is discussed elsewhere [5], [6].

Experimenting with coaxial IMPATT amplifiers revealed that both in-band and subharmonic spurious oscillations are a serious problem limiting the range over which the amplifiers can be operated. However, it should be possible with any given circuit to locate a slug position where spurious oscillations do not exist. During these experiments the utilization of a two-slug-tuned resonant cavity allowed sufficient circuit flexibility so that it was possible to achieve a tuning condition that eliminated all spurious oscillations, even when the diode was driven to saturation. This was accomplished by determining the circuit resonant frequencies as a function of slug positions over a frequency range extending from 4 to 12 GHz with the aid of a network analyzer. A slug position was located that minimized the number of circuit resonant frequencies, and this position was used to determine the amplifier operating frequency. This method, although resulting in a stable operating condition, has the disadvantage that it is not possible to select the optimum amplifier operating frequency, since this frequency is determined by the circuit parameters. However, it should be possible to design a stable amplifier for operation at any frequency by proper selection of the circuit parameters.

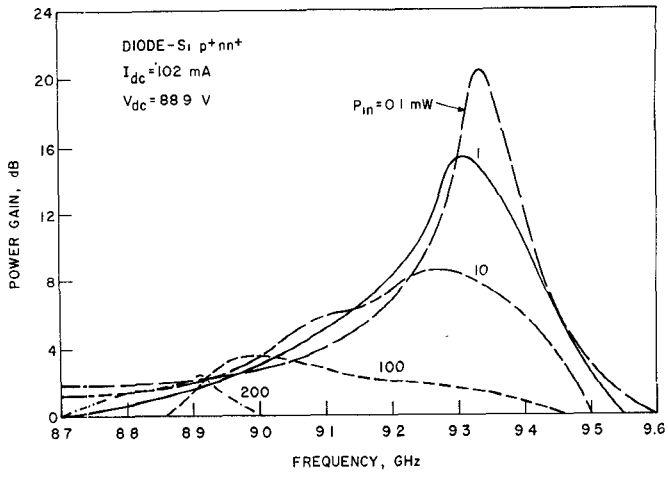

Fig. 3. IMPATT amplifier gain characteristics.

Results

Fig. 3 illustrates the gain characteristics of an amplifier tuned to provide 20.4 dB of small-signal gain at a frequency of 9.340 GHz. As expected, increasing the drive level resulted in a decrease in the maximum gain and its corresponding frequency. However, it is interesting to note that, at frequencies below the maximum gain frequency, it is possible to obtain increasing gain as a function of increasing drive level. This result is not entirely unexpected since, as Fig. 2 reveals, it is possible at low frequencies for the distance between common-frequency points on the diode and circuit negative-admittance curves to decrease with increasing drive level, and thus result in increasing gain over certain operating ranges. This behavior becomes more pronounced as the operating frequency of the amplifier approaches the avalanche frequency of the diode [3]. Increasing the drive level from small-signal operation to 200 mW of input power resulted in a decrease in maximum amplifier gain from 20.4 to 2.3 dB, while the maximum gain frequency was shifting from 9.340 to 8.910 GHz. The large-signal broad-band behavior of IMPATT operation is also demonstrated in Fig. 3. During these experiments no spurious oscillations were observed at any drive level.

The intermodulation measurements consist of two sets of tests: one with an input signal (F_1) fixed at the frequency of maximum small-signal gain, and the other input signal (F_2) set at higher frequencies defined by

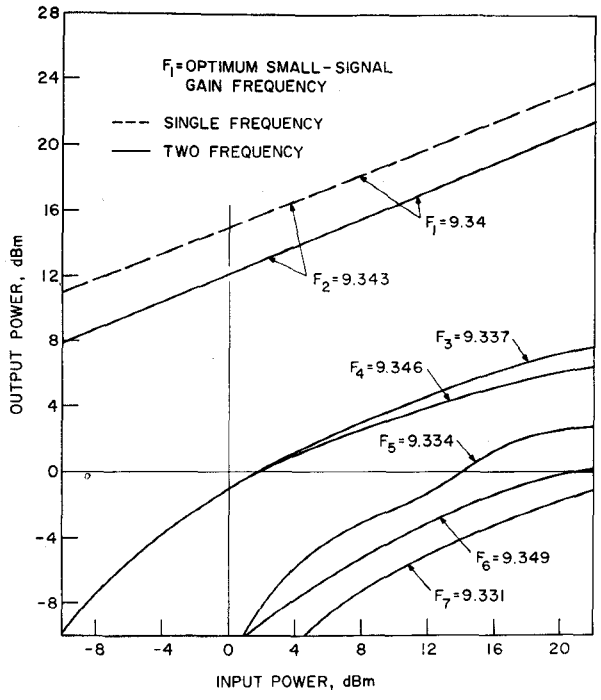

Fig. 4. Dynamic characteristics for IMPATT amplifier, 2 equal-amplitude input signals. ($\Delta f = 3$ MHz.)

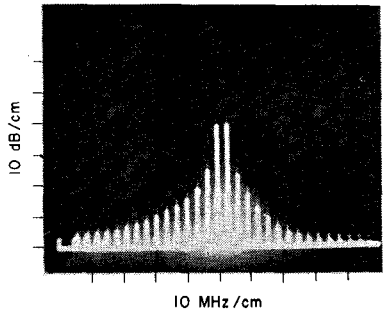

Fig. 5. Output spectrum for IMPATT amplifier, 2 equal-amplitude input signals. ($P_1 = P_2 = 100$ mW.)

frequency separations of 3, 10, 30, 100, and 200 MHz; and a second set of tests in which the input signal F_2 was fixed at the maximum small-signal gain frequency, and F_1 was set at lower frequencies defined by the above-frequency separations. Equal-amplitude input signals were used in all tests. Each test consisted of measurements of the amplifier output signals as a function of input drive levels first for single-frequency operation (only one input signal present at a time) and then for two-frequency (both input signals present) operation.

The $\Delta f = 3$-MHz test results of the first set of measurements are plotted in Fig. 4. At such small-frequency separations the gain is approximately constant, and therefore the same output power is generated in both fundamental signals. Applying both signals simultaneously to the amplifier input resulted in the generation of a complete spectrum of signals in the amplifier output (Fig. 5). For this work the intermodulation signals are defined as follows. First order: $F_3 = 2F_1 - F_2$, $F_4 = 2F_2 - F_1$. Second order: $F_5 = 3F_1 - 2F_2$, $F_6 = 3F_2 - 2F_1$. Third order: $F_7 = 4F_1 - 3F_2$. As expected, the power generated in the output of the fundamental signals was less for two-frequency operation than for single-frequency operation. The power difference appeared as power at the intermodulation frequencies, which have significant amplitudes even under small-signal operation. The first-order products F_3 and F_4 are the first to appear, and have the same magnitude until high drive levels are achieved where the shift of the gain characteristics favoring amplification at lower frequencies becomes significant. At the higher drive levels F_3 is amplified more than F_4 due to the gain shift. This effect is more apparent at the higher order intermodulation frequencies where the low-frequency product is always larger than its corresponding-order high-frequency counterpart. However, for $\Delta f = 3$-MHz operation, the largest intermodulation product F_3 is always at least 12 dB down from the fundamental signals.

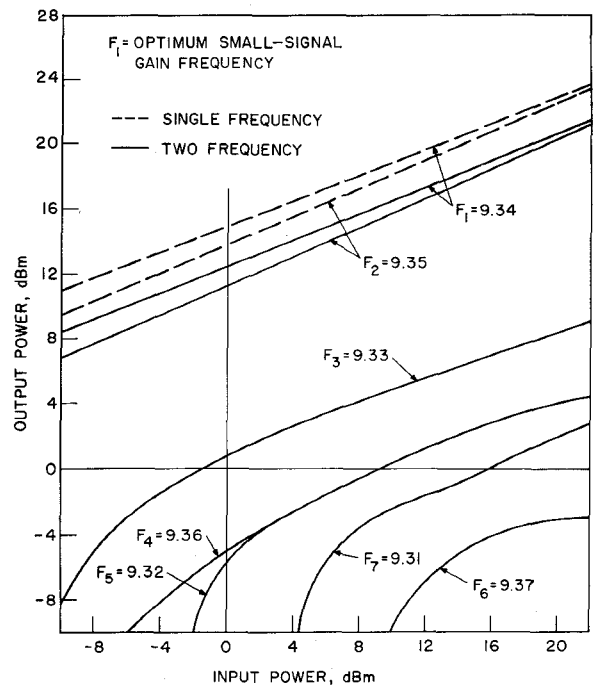

Fig. 6. Dynamic characteristics for IMPATT amplifier, 2 equal-amplitude input signals. ($\Delta f = 10$ MHz.)

Increasing the input-signal separation to 10 MHz (Fig. 6) results in the input signals no longer experiencing the same gain. The signal F_1 is always amplified more than F_2, although the two signals approach the same magnitude in the high drive-level limit. This behavior is similar for both single-frequency and two-frequency operation, and also holds for all frequency separations independent of their location relative to the gain characteristics. This result is expected due to the broad-band nature of the gain characteristics at high drive levels. In the $\Delta f = 10$-MHz test, F_3 is always the largest intermodulation product attaining a value within 10 dB of F_2. The low-frequency dominance

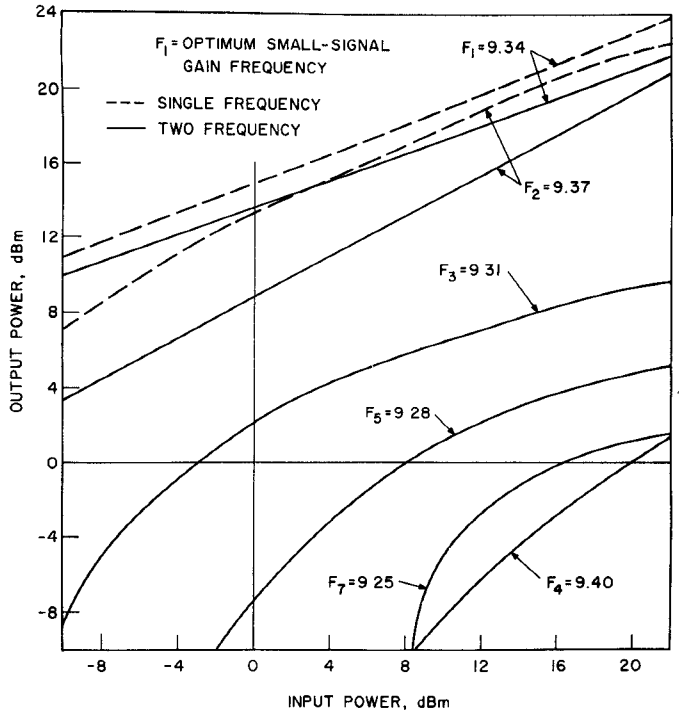

Fig. 7. Dynamic characteristics for IMPATT amplifier, 2 equal-amplitude input signals. ($\Delta f = 30$ MHz.)

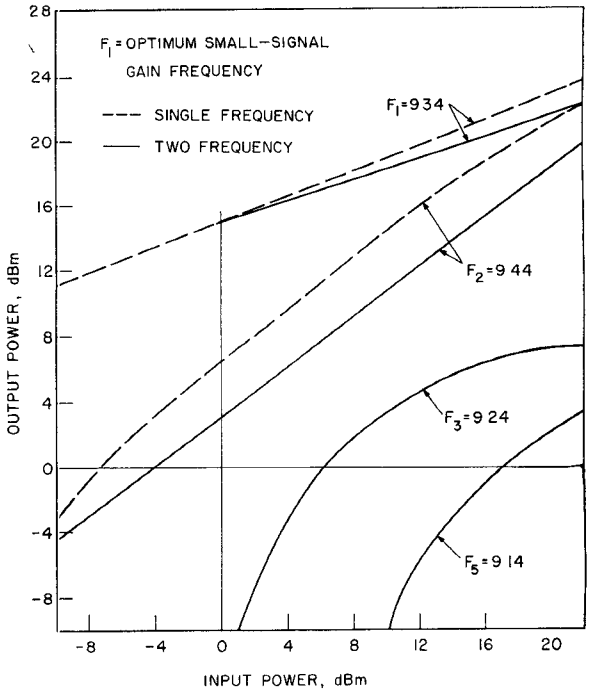

Fig. 8. Dynamic characteristics for IMPATT amplifier, 2 equal-amplitude input signals. ($\Delta f = 100$ MHz.)

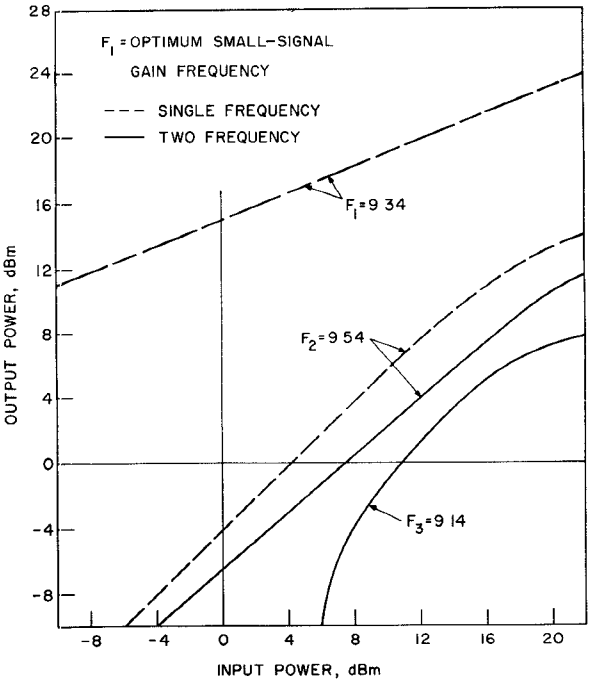

Fig. 9. Dynamic characteristics for IMPATT amplifier, 2 equal-amplitude input signals. ($\Delta f = 200$ MHz.)

mechanism is apparent in the higher order intermodulation products where the second-order low-frequency product F_5 is equal to the first-order high-frequency product F_4, and F_7 is always greater than F_6.

When the frequency separation is increased to 30 MHz (Fig. 7) it is observed that the high-frequency fundamental signal F_2 loses proportionately more power to the intermodulation products than the low-frequency fundamental signal F_1. This occurs because the gain shift to low frequencies with increasing drive level partially compensates for power lost to the intermodulation products by the low-frequency fundamental. In this test the first-, second-, and third-order low-frequency products all are larger than the first-order high-frequency product, with F_3 attaining a magnitude at one point within 7 dB of F_2.

Fig. 8 shows the results of the $\Delta f = 100$-MHz test. At this frequency separation, interaction between the two fundamental signals has decreased such that there are fewer intermodulation products generated. The low-frequency fundamental signal shows identical output power under single-frequency and two-frequency operation until higher drive levels are reached. The high-frequency fundamental signal F_2, however, because it experiences lower gain, generates considerably less power than signal F_1, and shows a power difference in the single-frequency and two-frequency results over the entire input power range. It is interesting to note that the gain of the two-frequency F_2 signal changes from a positive value to a negative value at an intermediate input power level, whereas the corresponding single-frequency gain is positive at all levels. The only significant intermodulation products generated are the low-frequency signals F_3 (which at one point is within 7 dB of F_2) and F_5.

Increasing the frequency separation to 200 MHz (Fig. 9) results in little interaction between the fundamental signals. The low-frequency signal F_1 shows iden-

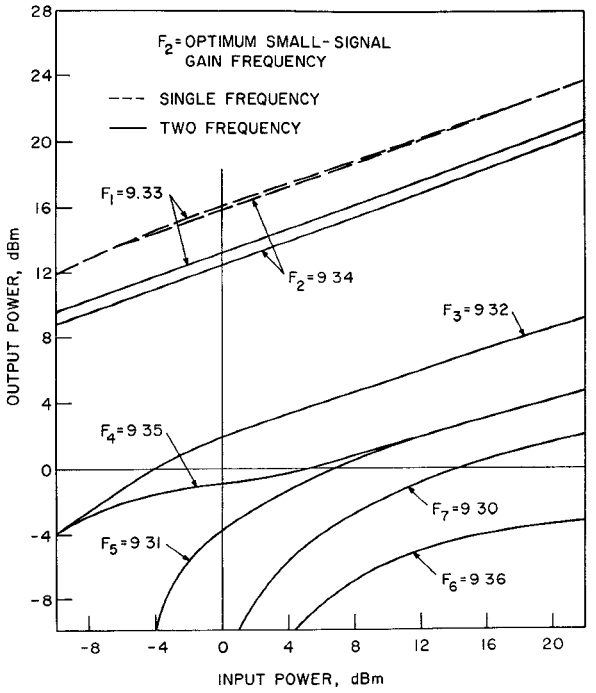

Fig. 10. Dynamic characteristics for IMPATT amplifier, 2 equal-amplitude input signals. ($\Delta f = 10$ MHz.)

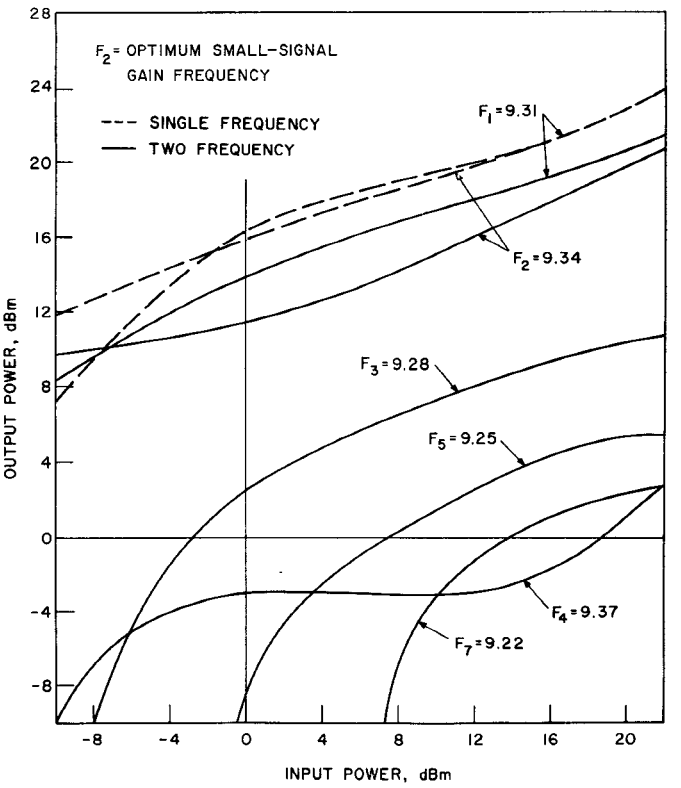

Fig. 11. Dynamic characteristics for IMPATT amplifier, 2 equal-amplitude input signals. ($\Delta f = 30$ MHz.)

tical single-frequency and two-frequency results. The only significant intermodulation signal to be generated (F_3) appears to obtain all its power at the expense of F_2 and attains a magnitude within 2 dB of that signal. No amplification is present at the F_2 frequency, however, as the gain of the F_2 signals is always negative.

When signal F_2 is set at the maximum small-signal gain frequency and the tests are repeated for different frequency values of F_1, the only significant difference observed in the $\Delta f = 3$-MHz test from that already discussed is that the intermodulation signals have greater magnitudes under small-signal operation. The greater magnitudes result from the peak gain shifting from the F_2 frequency through the F_1 and lower order intermodulation frequencies with increasing drive level. Due to the small frequency separations (3 MHz) this occurs under small-signal operating conditions.

Increasing the frequency separation to 10 MHz (Fig. 10) reveals a constant gain still present as the fundamental signals F_1 and F_2 both generate the same output power. Low-frequency dominance, however, is apparent as the low-frequency intermodulation products are generally larger in magnitude than their high-frequency counterparts.

The $\Delta f = 30$-MHz test (Fig. 11) clearly demonstrates the low-frequency dominance mechanism. When referring to the single-frequency curves it is seen that first F_2 and then F_1 have the greatest output magnitude. This behavior is explained by the shifting in the gain characteristics with increasing drive level. Since F_2 is fixed at the maximum small-signal gain frequency, it initially generates the greatest output power. However, as the drive level is increased, the peak gain frequency is lowered and passes through the F_1 frequency. As this occurs the greatest output power is generated in F_1, and the F_1 and F_2 curves cross over. Increasing the drive level further results in equal output power generated in the two signals as the large-signal broad-band behavior of the amplifier dominates. The two-frequency results indicate that the crossover of the F_1 and F_2 curves occurs at lower input power levels than the single-frequency results. This is due to the proportionately greater loss of power to the intermodulation products experienced by F_2. Since F_2 is initially the largest fundamental signal, F_4 is the first intermodulation product to appear. However, as the peak gain shifts through the low-frequency signals with increasing drive level, F_3, F_5, and F_7 all become larger than F_4.

Increasing the frequency separation to 100 MHz (Fig. 12) reveals that it is possible for the output power of one of the fundamental signals to actually decrease as the input drive level is increased. This is due to the increasing gain with increasing drive level present at the frequencies below the maximum small-signal gain frequency (Fig. 3). The relatively strong amplification of the low-frequency intermodulation signals requires significant power transferral from the fundamental signals. Due to the gain shift the high-frequency signal F_2 experiences a rapidly decreasing gain with increasing drive level, whereas the low-frequency fundamental and intermodulation signals all experience an increasing gain and

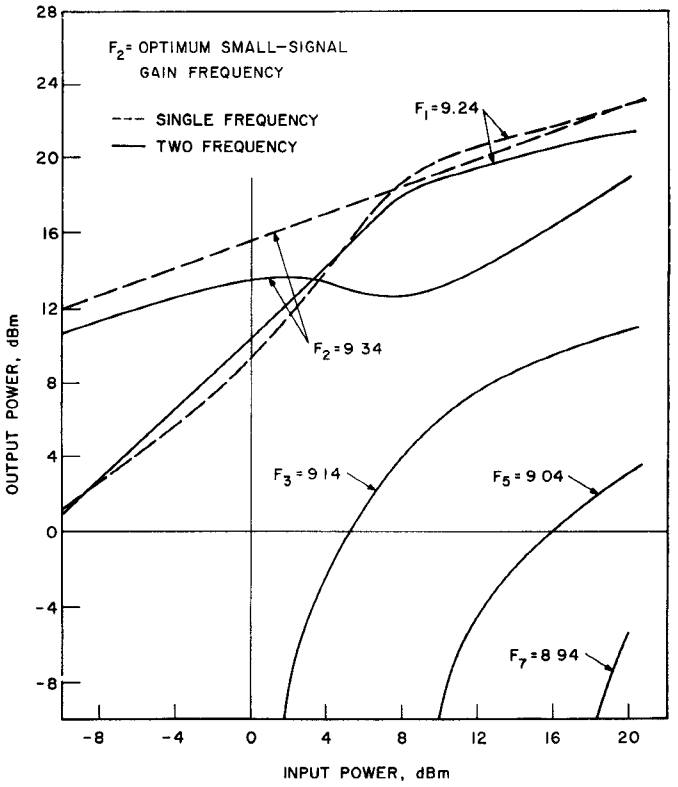

Fig. 12. Dynamic characteristics for IMPATT amplifier, 2 equal-amplitude input signals. ($\Delta f = 100$ MHz.)

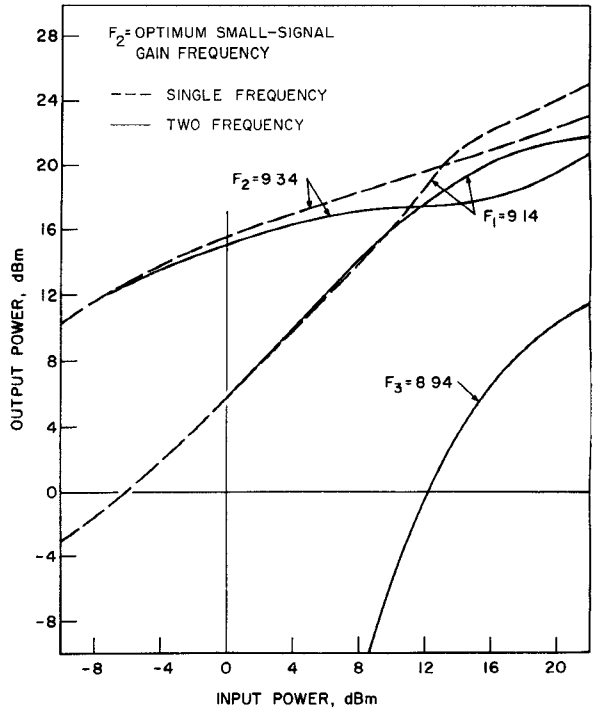

Fig. 13. Dynamic characteristics for IMPATT amplifier, 2 equal-amplitude input signals. ($\Delta f = 200$ MHz.)

then a slowly decreasing gain as the drive level is increased. Therefore, the high-frequency fundamental F_2 supplies most of the power generated at the intermodulation frequencies, and the result is a decrease in the output power of F_2 with increasing drive level over a portion of the operating range.

The $\Delta f = 200$-MHz test (Fig. 13) again indicates decreasing interaction between the two fundamental signals. Output power crossover is present, although at a greater input drive level than the preceding tests, and higher drive levels are required before a significant intermodulation product (F_3) is generated. When F_3 appears it shows a rapid generation of output power reaching a level within 8 dB of F_2.

Conclusions

Multisignal operation of IMPATT amplifiers results in the loss of available output power at the fundamental signals, with the power difference appearing in signals at intermodulation frequencies. IMPATT amplifiers are characterized by a decrease in the maximum gain and its corresponding frequency with increasing drive level providing a low-frequency dominance mechanism in which the low-frequency signals are amplified more than the high-frequency signals. The magnitude of the intermodulation signals is dependent upon both the nonlinear mixing properties of the IMPATT device and the passband characteristics of the amplifier. However, for small frequency separations between the fundamental signals (e.g., $\Delta f = 3$ MHz, $\Delta f = 10$ MHz), the signals experience approximately a constant gain, and the results are essentially independent of the amplifier passband behavior.

For larger frequency separations, especially at low drive levels, the test results become increasingly more a function of the passband characteristics. At high drive levels the influence of the passband behavior on the signal magnitudes is reduced due to the large-signal broad-band behavior of IMPATT amplifiers. However, the magnitude of the intermodulation signals is dependent to a greater extent upon the location of the signals relative to the amplifier gain characteristics than upon the frequency difference between the fundamental signals.

The experimental results indicate that it is possible for the first-, second-, and third-order low-frequency intermodulation products to have a greater magnitude than the first-order high-frequency product. Depending upon the location of the signals relative to the amplifier gain characteristics, it is possible for the largest intermodulation product F_3 to attain a magnitude within 2 dB of the smallest fundamental signal. Increasing the frequency separation between the fundamental signals results in less interaction between them such that there are fewer intermodulation products generated.

References

[1] P. T. Greiling and G. I. Haddad, "Large-signal equivalent circuits of avalanche transit-time devices," *IEEE Trans. Microwave Theory Tech. (Special Issue on Microwave Circuit Aspects of Avalanche-Diode and Transferred Electron Devices)*, vol. MTT-18, pp. 842–853, Nov. 1970.

[2] M. K. Scherba and J. E. Rowe, "Characteristics of multisignal and noise-modulated high-power microwave amplifiers," *IEEE Trans. Electron Devices*, vol. ED-18, pp. 11–34, Jan. 1971.
[3] R. W. Laton and G. I. Haddad, "The effects of doping profile on reflection-type IMPATT diode amplifiers," *Proc. 1971 European Microwave Conf.* (Stockholm, Sweden, Aug. 1971), pp. A 5/1:1–A 5/1:4.
[4] E. F. Scherer, "Large-signal operation of avalanche-diode amplifiers," *IEEE Trans. Microwave Theory Tech. (Special Issue on Microwave Circuit Aspects of Avalanche-Diode and Transferred Electron Devices)*, vol. MTT-18, pp. 922–932, Nov. 1970.
[5] W. E. Schroeder and G. I. Haddad, "Effect of harmonic and subharmonic signals on avalanche-diode oscillator performance," *IEEE Trans. Microwave Theory Tech.* (Corresp.), vol. MTT-18, pp. 327–331, June 1970.
[6] M. E. Hines, "Special problems in IMPATT diode power amplifiers," in *1972 IEEE Int. Solid-State Circuits Conf. Dig.* (Philadelphia, Pa., Feb. 1972), pp. 34–35.

18-GHz Paramps with Triple-Tuned Gain Characteristics for Both Room- and Liquid-Helium-Temperature Operation

TORU OKAJIMA, MASAHIKO KUDO, KIYOSHI SHIRAHATA, AND DAIJI TAKETOMI

Abstract—**The design and experimental performance of a wide-band K-band parametric amplifier (paramp) for the experimental domestic satellite communication earth station are described. An optimum idler frequency for a minimum noise temperature is derived taking into account the varactor diode skin effect. Wide-band paramps with a double-tuned signal circuit are discussed and it is shown that triple-tuned gain characteristics are realizable with this configuration. Finally, an 18-GHz paramp is described, which can be operated from room- to liquid-helium (LHe) temperature, only requiring adjustment of pumping power and bias voltage and using lithium ferrite circulators. Triple-tuned gain characteristics with a bandwidth of 1300 MHz at a gain of 10 dB are obtained using a miniature pill prong packaged varactor.**

I. Introduction

THE PAPER describes the design and experimental performance of a wide-band K-band paramp with both cryogenically cooled and room-temperature operation and intended for use in experiments on domestic satellite communication.

As the signal frequency is at K band and the idler frequency is in the millimeter wave region, skin effect in the varactor diode cannot be ignored, and the results obtained by Greene and Sard [1] must be modified.

A design technique to maximize the voltage gain-bandwidth product of a single-tuned paramp has been presented [2]. Design techniques on paramps with a double-tuned signal circuit have been also represented by DeJager [3] and Connors [4], and conditions to obtain maximally flat gain characteristics have been included therein. However, these conditions are restrictive in that the paramp gain cannot be chosen at will after other parameters of the paramp have been established. Getsinger [5] has presented the requirements on second signal resonator Q for obtaining wide-band gain characteristics as a function of the gain ripple and the single-tuned bandwidth. Because an equivalent circuit of single-tuned paramps cannot always be entirely represented by a negative resistance and positive reactance elements, these results are sometimes difficult to apply.

Broad-band matching of a parametric amplifier by the network synthesis method has been presented by Porra and Somervuo [6]. But this paper intends to derive the broad-banding factor, the shape of the resulting gain characteristics, and the required Q of the second signal resonator for paramps with a double-tuned signal circuit in terms of given single-tuned paramps.

The required noise temperature for a K-band paramp system is about 100 K based upon the antenna noise temperature considerations. This noise temperature

Manuscript received May 15, 1972; revised July 24, 1972. This paper was presented at the 1972 International Microwave Symposium, Chicago, Ill., May 22–24, 1972.

T. Okajima is with Musashino Electrical Communication Laboratory, Nippon Telegraph and Telephone Public Corporation, Musashino City, Japan.
M. Kudo is with the Microwave Division, Nippon Telegraph and Telephone Public Corporation, Tokyo, Japan.
K. Shirahata and D. Taketomi are with Kamakura Works, Mitsubishi Electric Corporation, Kamakura City, Japan.